"Forbidden" Four-Center Reactions: Molecular Orbital Considerations for $N_2 + N_2$ and $N_2 + N_2^+$

F. Matthias Bickelhaupt,[†] Roald Hoffmann,* and Raphael D. Levine[‡]

Baker Laboratory, Department of Chemistry, Cornell University, Ithaca, New York 14853-1301

Received: March 20, 1997; In Final Form: July 2, 1997[⊗]

The hypothetical four-center nitrogen exchange reaction of $N_2 + N_2$ is analyzed. We show that the three level crossings accompanying the least-motion nitrogen exchange reaction occur at different points along the reaction coordinate, leading to a mechanism requiring three "singly forbidden" reaction steps. Simple MO arguments show that the loss of one electron in $N_2 + N_2^+$ reduces the energy demand associated with the energetically dominating first and third level crossing, suggesting that ionization of the reaction system lowers significantly the high activation barrier. This is supported by nonlocal density functional calculations on various N_4 and N_4^+ structures, which, however, also indicate that the barrier still remains at high energy: the tetraazacyclobutadiene intermediate involved in the neutral reaction is 166.7 kcal/mol higher in energy than $N_2 + N_2$; the corresponding radical cation is only 52.2 kcal/mol above $N_2 + N_2^+$. The DFT results also indicate that the $N_2 + N_2^+$ nitrogen exchange reaction, if it occurs at all, may also proceed via a competing mechanism involving a T-shaped transition state at 102.8 kcal/mol above $N_2 + N_2^+$. Suggestions for further experimental investigations emerge from this analysis.

1. Introduction

Early work in molecular reaction dynamics emphasized simple atom exchange reactions, ones where the old bond is breaking, while the new bond is forming, in concert. Pioneering studies of four-center reactions, where two bonds are broken and two new bonds are formed, were limited to facile reactions involving ionic reactants and products.[1] Currently, there is an increasing interest in more complicated reactions, where more than one bond is broken or formed. For these multicentered reactions we need to know more about the topography of the potential energy surface, and one may well expect that there is more than one barrier separating reactants and products,[2] so that different pathways may be possible[3] for the same reaction.

Current experimental research also provides hitherto unavailable opportunities for examination of the dynamics of reaction over high barriers. One can use translationally hot reactants,[4] or vibrationally hot ones.[5] One can form hot reactants by femtosecond excitation,[3a,3d] which allows probing the dynamics in real time. One can also speculate about other means of ultrafast heating.[6] When a reactant is charged, one can, of course, more readily control the kinetic energy of the collision.[7] It is, therefore, also appropriate to examine higher barrier reactions than was possible in the earlier days.

Four-center reactions are expected to have high barriers. We illustrate this well-known expectation with the hypothetical nitrogen exchange reaction (eq 1):

$$N{\equiv}N + {}^*N{\equiv}N^* \rightleftarrows 2\ N{\equiv}N^* \qquad (1)$$

Here, * marks an isotopic label. As shown in Figure 1, the bimolecular least-motion process has no less than three level crossings in its level correlation diagram.[8,9]

One would call the reaction triply forbidden. One could envisage other, "less forbidden", lower symmetry processes, or a termolecular one through a high energy benzenoid N_6. But all of these are still likely to be of high energy.

Our purpose in this article is 2-fold. The first is that we want to elaborate on this immediate characterization of the N_2 exchange reaction as a highly forbidden one. Do all three crossings occur at about the same location along the reaction coordinate? And how far can one go with qualitative considerations in understanding the nature of the barrier to reaction? We then confirm the more qualitative discussion with quantitative computations using a nonlocal density functional approach.

The second purpose is to explore the required condition for reaction if one of the partners is ionized. In a number of other four atom reactions (e.g., in $N_2 + H_2^+$ and $N_2^+ + H_2$,[10] or in the neutral but isoelectronic $CN + H_2$ reaction[11]) there is a dramatic lowering of the barrier. We were therefore led to study the $N_2 + N_2^+$ reaction. This, in turn, led us to consider various N_4 and N_4^+ isomers **1**−**10** (the drawings below schematically indicate geometries, not valence structures; the computed optimum geometries will be given later):

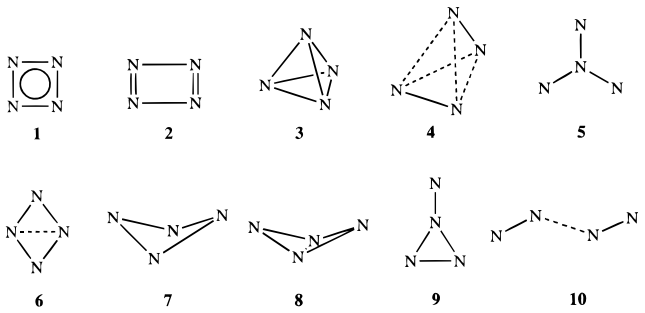

It is also becoming realistic to study the alternative roles of vibrational and translational excitation of the reactants. The interpretation of such effects requires an understanding of the topography of the potential energy surface(s) away from the minimum energy path. The various isomers that we consider also provide a preliminary foray in this direction. In particular, we note that for kinematic reasons[6] four-center reactions may require a stretching of the old bonds in order for reaction to

[†] Present address: Fachbereich Chemie, Philipps-Universität Marburg, Hans-Meerwein-Strasse, D-35032 Marburg, Germany.

[‡] The Fritz Haber Research Center for Molecular Dynamics, The Hebrew University of Jerusalem, Jerusalem, 91904, Israel.

[⊗] Abstract published in *Advance ACS Abstracts,* October 15, 1997.

S1089-5639(97)01005-0 CCC: $14.00

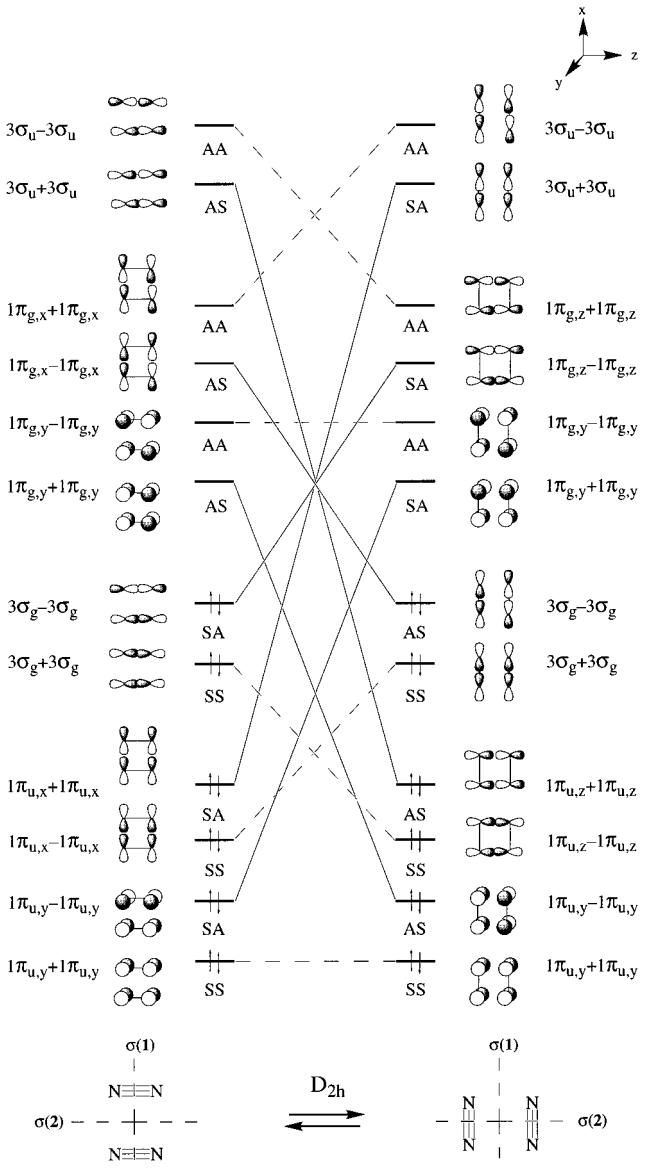

Figure 1. Orbital correlation diagram for the exchange reaction between two nitrogen molecules approaching in a parallel manner with D_{2h} geometry. The levels, given as combinations of the N_2 orbitals, are either symmetric (S) or antisymmetric (A) with respect to the mirror planes $\sigma(1)$ and $\sigma(2)$.

take place. It is interesting, therefore, to consider nonsquare configurations. For discussing whether both the new bonds form in concert or sequentially,[3] knowledge of more distorted configurations is required. Finally, there is the question of whether the reaction proceeds at all via a four-center-like transition state since, say, a T-shaped or even an L-shaped configuration can also be envisaged, nor is it obvious that the transition state has to be planar.

Neutral N_4 isomers have been the subject of previous theoretical studies, both because of their significance in such fundamental chemical concepts as ring strain and aromaticity and also because of the potential application of tetraazatetrahedrane (**3**) as a high energy density material.[12] Experimental[17a,13] and previous theoretical[14] investigations on N_4^+ were prompted, among others, by its involvement in stratospheric chemistry.

The molecules and reactants under consideration were studied with high-level density functional theoretical (DFT) methods[15] using the ADF program.[16,17] The DFT computations, in particular a detailed analysis of the bonding mechanism in neutral and cationic tetraazacyclobutadiene (**2**), mainly serve to support the qualitative MO arguments. The uniform treatment of neutral and cationic N_4 isomers in our DFT calculations allows, furthermore, for a direct comparison between corresponding structures and energetics. The present study, therefore, also contributes to our quantitative knowledge of N_4 and N_4^+ species.

2. Method

A. General Procedure. All DFT calculations were performed using the Amsterdam-density-functional (ADF) program.[16,17] The MOs were expanded in a large uncontracted set of Slater type orbitals (STOs) containing diffuse functions: TZ2P (no Gaussian basis functions are involved).[16c] The nitrogen basis set is of triple-ζ quality, augmented with a set of 3d and 4f polarization functions. The 1s core shell was treated by the frozen-core approximation.[16a,16b] An auxilliary set of s, p, d, f, and g STOs was used to fit the molecular density and to represent the Coulomb and exchange−correlation potentials accurately in each self-consistent-field (SCF) cycle.[16a] The numerical integration was performed using the procedure developed by te Velde et al.[16d]

Equilibrium geometries and energies were optimized at the nonlocal SCF (NL-SCF) level. Frequencies were calculated using the local density approximation (LDA). At the LDA, level exchange is described by Slater's Xα potential[15b] and correlation is treated in the Vosko−Wilk−Nusair (VWN) parametrization.[16e] At the NL-SCF level, nonlocal corrections for the exchange due to Becke[16f,g] and for correlation due to Perdew[16h] are added self-consistently.[16i] Energies are calculated directly *with respect to atoms* in *one* numerical integration of the difference energy density $\epsilon[\rho,\mathbf{r}] - \sum_A \epsilon_A[\rho,\mathbf{r}]$ between the overall molecule and the composing atoms: $\Delta E[\rho] = \int \epsilon[\rho,\mathbf{r}] - \sum_A \epsilon_A[\rho,\mathbf{r}]\, d\mathbf{r}$. In other words, we evaluate the energy of the overall molecule, $E[\rho] = \int \epsilon[\rho,\mathbf{r}]\, d\mathbf{r}$, and the energies of each of the composing atoms, $E_A = \int \epsilon_A[\rho,\mathbf{r}]\, d\mathbf{r}$, in *the same* numerical integration grid. This provides more accurate relative energies than subtracting total energies from separate calculations, because the same relative numerical integration error applies to a much smaller quantity, yielding in turn a much smaller absolute error.

B. Bond Analysis. The extended transition state (ETS) method developed by Ziegler and Rauk[17] was used for a more detailed analysis of the bonding between dinitrogen fragments in the D_{2h} symmetric species **2** and $\mathbf{2}^+$. The overall bond energy ΔE is divided into two major components (eq 2):

$$\Delta E = \Delta E_{\text{prep,geo}} + \Delta E_{\text{prep,el}} + \Delta E_{\text{int}} = \Delta E_{\text{prep}} + \Delta E_{\text{int}} \quad (2)$$

The preparation energy ΔE_{prep} is the amount of energy required to deform the separated fragments from their equilibrium structure to the geometry that they acquire in the overall molecule ($\Delta E_{\text{prep,geo}}$) and to excite them to the their valence electronic configuration ($\Delta E_{\text{prep,el}}$). The next step of the ETS bond analysis is the calculation of the interaction energy ΔE_{int}. This is done by calculating the energy of the composite molecule with respect to that of the prepared fragments.[17] E_{int} can be further split up into two physically meaningful terms (eq 3):

$$\Delta E_{\text{int}} = \Delta E_{\text{elst}} + \Delta E_{\text{Pauli}} + \Delta E_{\text{oi}} = \Delta E^0 + \Delta E_{\text{oi}} \quad (3)$$

Here, ΔE_{elst} corresponds to the classical electrostatic interaction between the unperturbed charge distributions of the prepared fragments and is usually attractive. The Pauli repulsion ΔE_{Pauli} comprises the four-electron destabilizing interactions between occupied orbitals and is responsible for any steric repulsion. For neutral fragments, it is useful to combine ΔE_{elst} and ΔE_{Pauli} in the steric interaction ΔE^0 (eq 3). The orbital interaction ΔE_{oi} accounts for electron-pair bonding, charge transfer (e.g. HOMO−LUMO interactions), and polarization (empty/occupied orbital

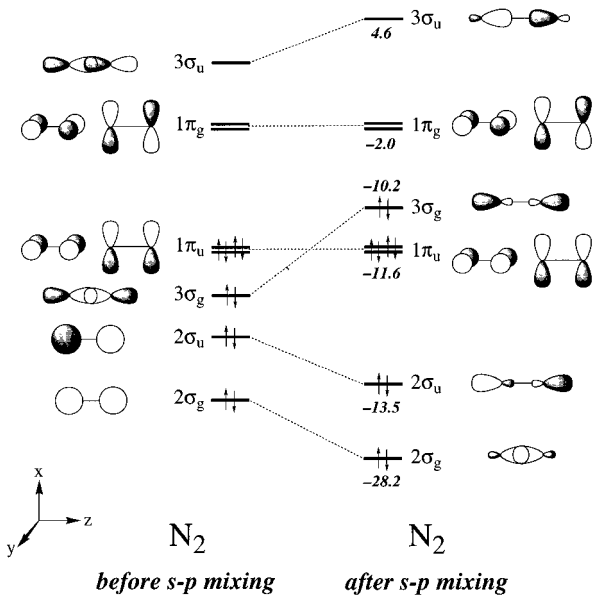

Figure 2. Valence MO scheme of the nitrogen molecule before (to the left) and after s−p mixing (to the right) with orbital energies in eV.

mixing on one fragment due to the presence of another fragment).

3. Results and Discussion

A. Nitrogen Molecule. The nitrogen molecule is the basic fragment in the nitrogen exchange reaction. Its familiar valence MOs are schematically depicted in Figure 2. At the bottom, we have the $2\sigma_g$ and $2\sigma_u$ orbitals which to zeroth order are $2s_A + 2s_B$ and $2s_A - 2s_B$ (i.e. the bonding and antibonding combinations of the nitrogen 2s AOs; Figure 2, before s−p mixing) with a first-order (in wave functions) admixture of $2p_{z,A} - 2p_{z,B}$ and $2p_{z,A} + 2p_{z,B}$ (Figure 2, after s−p mixing). The same s−p mixing destabilizes both $3\sigma_g$ and $3\sigma_u$, which to zeroth order are $2p_{z,A} - 2p_{z,B}$ and $2p_{z,A} + 2p_{z,B}$, assuming a coordinate system $\vec{z}$,A $\vec{z}$,B. As a result, $3\sigma_g$ is pushed up in energy between $1\pi_u$ and $1\pi_g$, the bonding and antibonding combinations of the $2p_x$ and $2p_y$ AOs on each nitrogen. $3\sigma_g$ is thus higher in energy than π_u despite the larger σ type overlap between two 2p orbitals.[9] Another way to describe the orbitals after second-order mixing is that $2\sigma_g$ becomes the N−N σ bond, $3\sigma_u$ the corresponding σ^*, and $2\sigma_u$ and $3\sigma_g$ the out-of-phase and in-phase combinations of N lone pairs. This well-known N_2 orbital pattern is confirmed by our NL-SCF/TZ2P calculations (Figure 2).

B. Neutral Nitrogen Exchange. Next, we consider the neutral $N_2 + N_2$ nitrogen exchange reaction. In this bimolecular process, the nitrogen molecules can approach in several relative orientations, all of which could, in principle, lead to nitrogen exchange. The most obvious approach is probably the parallel approach which would proceed via square or rectangular intermediates or activated complexes, such as **1** or **2**. "Perpendicular" approaches passing through (distorted) tetrahedral (**3** or **4**) or Y-shaped structures (**5** or **9**) are also conceivable.

While the orbital details differ, the overall transformation is in all these cases "triply forbidden", just as was shown in some detail for the least-motion process in Figure 1.[18] However, do the three level crossings in Figure 1 really occur, more or less, at the same point along the reaction coordinate? We try to answer this question through a qualitative MO analysis of the parallel approach of two nitrogen molecules, with some help from the DFT calculations. The latter were applied to several of the pathways suggested above. The computed relative energies are presented in Table 1, and the calculated equilibrium geometries of various intermediates in Figure 3.

What happens to the orbitals of two nitrogen molecules that approach in a parallel manner with D_{2h} geometry? It turns out in the calculations that the level crossings are staged and lag behind each other. First, one obtains an intermediate tetraazacyclobutadiene structure **2** (eq 4). In agreement with previous calculations,[12] **2** is a stable intermediate; we find it at 166.7 kcal/mol above the reactants (Table 1, Figure 3b). An estimate for the activation energy is ca. 172 kcal/mol,[12m] with an upper bound of 307.8 kcal/mol, as will be explained in section 3D.

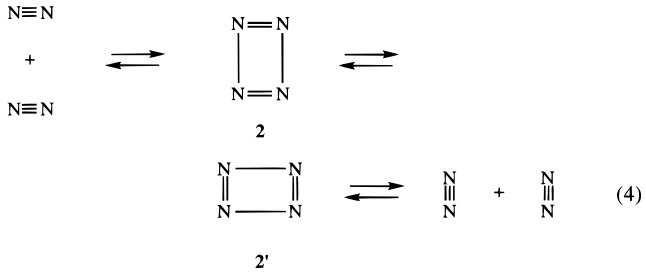

(4)

The next level crossing takes place as the system passes from

TABLE 1: NL-SCF/TZ2P Relative Energies (kcal/mol) of Neutral and Cationic N_4 Systems in Comparison with Literature Data[a]

system		neutral multipl	NL-SCF[b]	NL-SCF[c]	HF[d]	MP2[d]	MP4SDTQ[d]	G2[e]	cationic multipl	NL-SCFf
$2N_2$[g]	$D_{\infty h}$	s	0.0 (0)	−157.9 (0)			−182.8[h]	−177.4	d	0.0 (0)
1	D_{4h}	t	184.0 (1)	26.1 (1)	−8.8 (3)	35.3	26.3[i]		q	102.9
2	D_{2h}	s	166.7 (0)	8.8 (0)	−9.0 (0)	12.4 (0)	1.1	2.7	d	52.2 (0)
3	T_d	s	157.9 (0)	0.0 (0)	0.0 (0)	0.0 (0)	0.0	0.0	d	127.9
4	D_{2d}	s	*j*	*j*					d	90.7 (0)
5	D_{3h}	t	226.5 (0)	68.6 (0)	97.6 (0)	138.5			q	138.6
6	D_{2h}	t	191.8 (1)	33.9 (1)					q	94.5
7	D_{2d}	t	174.2 (1)	16.3 (1)	−12.8 (2)	29.6 (0)	17.6		d	88.7
8	C_{2v}	t	*k*	*k*					d	76.7 (1)
9	C_{2v}	s	171.3 (1)	13.4 (1)	8.9 (0)	20.9 (1)	13.6[i]		d	35.4 (1)
10	chain[l]	t	130.7 (0)	−27.2 (0)	−73.9 (0)	0.1 (0)	−20.6	−20.8	d	−46.7 (0)[m,n]

[a] Number of imaginary frequencies in parentheses; DFT frequencies calculated at LDA/TZ2P. multipl = multiplicity: singlet (s), doublet (d), triplet (t), quartet (q). [b] This work: NL-SCF/TZ2P relative to $2N_2$. [c] This work: NL-SCF/TZ2P relative to **3**. [d] HF/6-31G*, MP2/6-31G*, MP4SDTQ(fc)/6-311+G*//MP2/6-31G*; ref 12f. [e] Reference 12b. [f] This work: NL-SCF/TZ2P relative to $N_2 + N_2^{\bullet+}(^2\Sigma_g^+)$, which is 355.8 kcal/mol above $2N_2$. We find $N_2^{\bullet+}(^2\Pi_u)$ 27.3 kcal/mol above ground-state $N_2^{\bullet+}(^2\Sigma_g^+)$ (see section 3E). [g] N_2 = ground-state $N_2(^1\Sigma_g^+)$. Triplet $N_2(^3\Sigma_u^+)$ is 148.9 kcal/mol higher in energy at NL-SCF/TZ2P (see section 3E). [h] MP4SDTQ(fc)/6-31G**//MP2/6-31G**. [i] MP4SDTQ(fc)/6-31G*//MP2/6-31G*. [j] Starting geometry of D_{2d} symmetry converges to T_d structure **3**. [k] Starting geometry of C_{2v} symmetry converges to D_{2d} structure **7**. [l] Neutral: C_{2h}; cationic: $D_{\infty h}$. [m] −40.1 at HF/6-31G*, 8.2 at MP2/6-31G*, and −29.7 kcal/mol at QCISD/6-31G*, ref 14a. [n] PIPECO experiments: −25.1 kcal/mol, ref 13a.

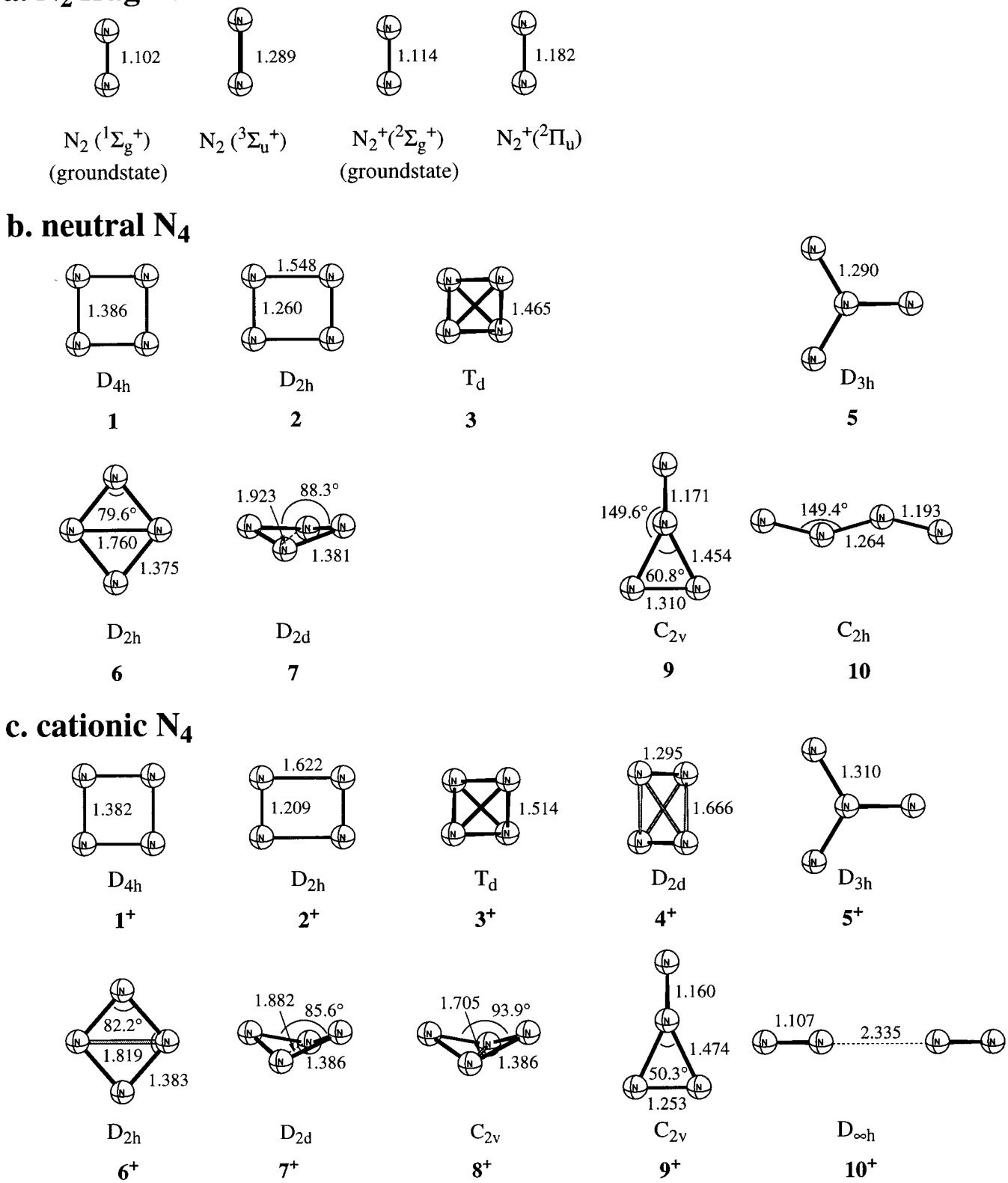

Figure 3. NL-SCF/TZ2P optimized geometries (Å, deg) of N_4 and N_4^+ systems.

one D_{2h} **2** through the Jahn−Teller unstable square D_{4h} to **2′**, also D_{2h}. The D_{4h} way-point is at high energy (eq 4). A triplet (**1**, $d_{NN} = 1.386$ Å) is at 184 kcal/mol above $2N_2$. This energy is a lower bound for the actual activation energy on the singlet potential energy surface (PES). An upper bound is provided by the two "Jahn−Teller unstable" configurations, which we compute to be at 206 kcal/mol.

The third level crossing is the "reverse" of the first one. What is important is that the three level crossings in this four-center nitrogen exchange definitely take place sequentially. They are three "singly forbidden" steps.

C. Cationic Nitrogen Exchange. Ionization of $N_2 + N_2$ brings us to the cationic nitrogen exchange reaction (eq 5):

$$N{\equiv}N^+ + {}^*N{\equiv}N^* \rightleftarrows N{\equiv}N^{*+} + N{\equiv}N^* \qquad (5)$$

How does this reaction differ from the corresponding neutral one (eq 1), discussed in the previous paragraph? The orbital

correlation diagram is qualitatively very similar: there are again three level crossings, suggesting a three-step mechanism with two equivalent intermediates, $\mathbf{2}^+$ and $\mathbf{2'}^+$, connected via a D_{4h} symmetric transition state. The existence of the tetraazacyclobutadiene cation $\mathbf{2}^+$ as a true energy minimum is confirmed by the DFT computations (Table 1 and Figure 3).

The main difference with respect to the neutral reaction is that the HOMO is lacking one of its electrons and that, as consequence, only *one* electron instead of two is involved in the empty−occupied level crossings of the first and the last reaction step, which therefore become roughly 2 times less energy-demanding (see below):

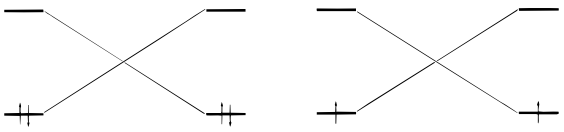

The situation in the second reaction step is somewhat different. Here we have to consider both the empty−occupied level crossing of the π orbitals $1\pi_{u,y} - \pi_{u,y}$ and $1\pi_{g,y}+1\pi_{g,y}$ and the level crossing of the occupied lone-pair orbitals $3\sigma_g - 3\sigma_g$ and $1\pi_{g,x} - 1\pi_{g,x}$ (see Figure 1). In the neutral system, the lone-pairs were either higher (in **2** and **2′**) or essentially at the same energy (in **1**) as the occupied π orbitals (vide supra). This suggests that ionization leads to the removal of a lone-pair electron. As a consequence, the empty−occupied π level crossing is unaffected, whereas the four-electron occupied level crossing of the lone-pairs turns into an energetically more demanding three-electron level crossing (see below):

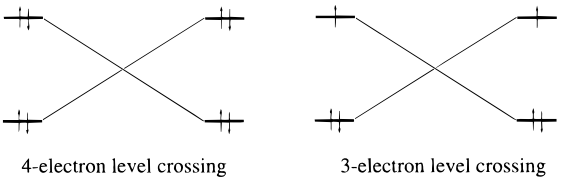

The transformation of $\mathbf{2}^+$ into $\mathbf{2'}^+$ is thus accompanied by a two-electron empty−occupied as well as a three-electron orbital level crossing; it is, so-to-say, "1.5-fold forbidden".

We conclude that ionization turns the nitrogen exchange reaction from a sequence of three singly forbidden reaction steps into one that consists of a "*half* forbidden" cycloaddition, a "1.5-fold forbidden" isomerization, and a "*half*-forbidden" reverse cycloaddition. The reduction of the very high first and third barriers by roughly a factor 2 probably dominates the increase of the smaller second barrier. We expect thus that the overall barrier decreases upon ionization.

The DFT results support our qualitative arguments. Intermediate **2** is at 166.7 kcal/mol with respect to $N_2 + N_2$, whereas $\mathbf{2}^+$ is only 52.2 kcal/mol above the reactants $N_2^+ + N_2$. This suggests that the barrier to nitrogen exchange is dramatically lowered upon ionization. The approximate barrier for the cycloaddition step is indeed reduced from ca. 154 to ca. 91 kcal/mol; the corresponding upper bounds are 307.8 and 181.9 kcal/mol, respectively (see section 3D).

The barrier associated with the second reaction step increases with respect to the intermediates (**2**, $\mathbf{2}^+$), but with respect to the reactants ($N_2 + N_2$, $N_2 + N_2^+$) it is also significantly reduced. The ground state of the D_{4h} symmetric species is a quartet with configuration $(3\sigma_g - 3\sigma_g)^2\ (1\pi_{g,x} - 1\pi_{g,x})^1\ (1\pi_{u,y} - 1\pi_{u,y})^1\ (1\pi_{g,y}+1\pi_{g,y})^1$. The quartet species $\mathbf{1}^+$ is 102.9 kcal/mol above the reactants $N_2 + N_2^+$ (Table 1). This is a lower bound for the activation energy on the doublet PES. The energy associated with each of the two "Jahn−Teller unstable" configurations, i.e. $(1\pi_{u,y} - 1\pi_{u,y})^2\ (1\pi_{g,y} + 1\pi_{g,y})^0$ or $(1\pi_{u,y} - 1\pi_{u,y})^0\ (1\pi_{g,y} + 1\pi_{g,y})^2$, is an upper bound for the barrier. Using the geometry of $\mathbf{1}^+$, we find it at 130.5 kcal/mol above the reactants. Note that this upper bound value is beneath the lower bound of 184.0 kcal/mol for the corresponding neutral reaction. Note however also that with respect to the intermediates the lower bound value for the barrier of step 2, i.e. the energy of **1** ($\mathbf{1}^+$) relative to **2** ($\mathbf{2}^+$), increases upon ionization from 17.3 to 50.7 kcal/mol.

TABLE 2: Analysis of the N_2-N_2 Bond in Rectangular N_4 and N_4^+ in the Geometry of 2^+ [a]

	N_4	N_4^+
	Energy (kcal/mol)[b]	
ΔE_{Pauli}	295.0	248.6
ΔE_{elst}	−120.9	−63.8
ΔE_{oi}	−308.0	−314.5
ΔE_{int}	−133.9	−129.7
$\Delta E_{prep,geo}$	29.2	25.7
$\Delta E_{prep,el}$	278.6[b]	156.2[b]
ΔE	173.9	52.2
	Fragment Orbital Overlaps[c]	
$\langle 3\sigma_g \vert 3\sigma_g\rangle$	0.16	0.08
$\langle 1\pi_{u,x} \vert 1\pi_{u,x}\rangle$	0.25	0.25
$\langle 1\pi_{u,y} \vert 1\pi_{u,y}\rangle$	0.16	0.14
$\langle 1\pi_{g,x} \vert 1\pi_{g,x}\rangle$	0.23	0.23
$\langle 1\pi_{g,y} \vert 1\pi_{g,y}\rangle$	0.16	0.14
$\langle 3\sigma_u \vert 3\sigma_u\rangle$	0.54	0.48
	Fragment Orbital Populations (el)[d]	
$3\sigma_g$	1.80	1.82[e]
$1\pi_{u,x}$	1.18	1.17[e]
$1\pi_{u,y}$	2.00	2.00/1.98[e]
$1\pi_{g,x}$	1.01	0.59[e]

[a] NL-SCF/TZ2P. [b] See section 2, eqs 2 and 3; $\Delta E_{prep,el}(N_2) = 139.3$ kcal/mol; $\Delta E_{prep,el}(N_2^+) = 16.9$ kcal/mol. [c] Overlaps between orbitals of $N_2 + N_2$ or $N_2 + N_2^+$ fragments. [d] Gross Mulliken population which a fragment orbital carries in the overall molecule. [e] N_2 orbital population/N_2^+ orbital population. A single value is given if both populations are equal.

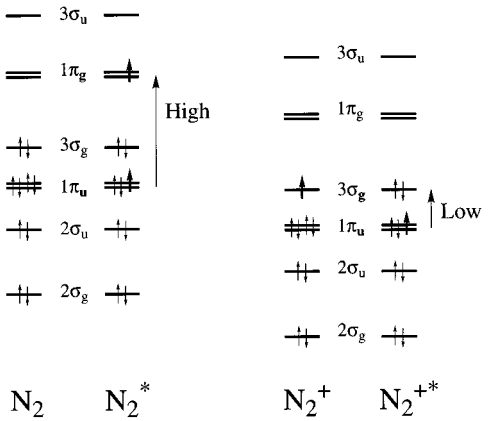

Figure 4. Electron configurations of the nitrogen molecule (left) and its radical cation (right) in the ground state (N_2 and N_2^+) and in the valence state they acquire in **2** and $\mathbf{2}^+$ (N_2* and N_2^+*). Note that achieving the valence state is associated with a high-energy excitation for N_2 and a low-energy excitation for N_2^+.

D. Quantitative Analysis of the Electronic Structure. Intrigued by the dramatic fall in activation energy upon ionization, we have analyzed the N_2-N_2 bond in more detail to understand why, upon ionization, the intermediate is so enormously stabilized with respect to the reactants (Table 2, Figures 4 and 5). To enable a direct comparison, the neutral intermediate **2** was slightly deformed to structure **2a**, which has

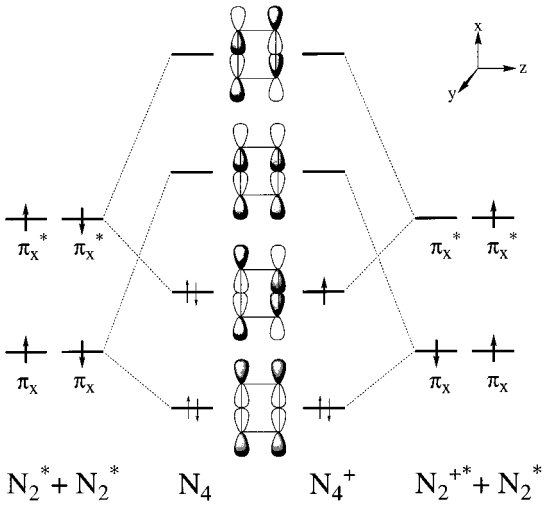

Figure 5. Orbital interactions between N_2* and N_2* in **2** and between N_2* + N_2^+* in $\mathbf{2}^+$.

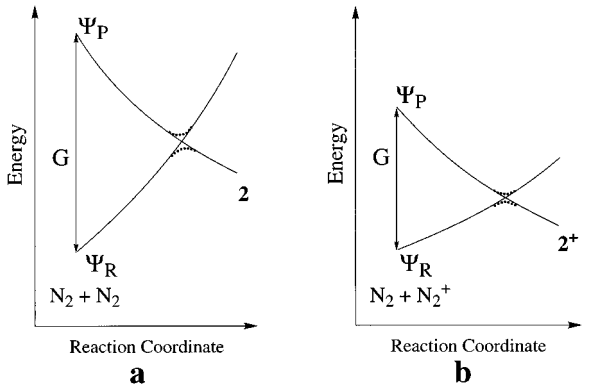

Figure 6. Curve-crossing model for the reactions $N_2 + N_2 \rightarrow$ **2** (a) and $N_2 + N_2^+ \rightarrow \mathbf{2}^+$ (b). Ψ_R and Ψ_P are the reactant and product configurations; in the reactants, they are separated by an energy gap *G*. Configuration mixing near the crossing point causes an avoided crossing (dotted line).

the same geometry as $\mathbf{2}^+$; **2a** is only 7.2 kcal/mol higher energy than **2**.

The valence configuration of the slightly elongated dinitrogen fragments N_2* in **2a** corresponds to an excited state of N_2: one electron of the bonding $1\pi_{u,x}$ has been excited to the antibonding $1\pi_{g,x}$ (Figure 4). This excitation reflects the level crossing between $1\pi_{u,x} - 1\pi_{u,x}$ and $1\pi_{g,x} + 1\pi_{g,x}$; it is associated with a relatively high excitation energy of 139.3 kcal/mol per N_2 or $\Delta E_{prep,el} = 278.6$ kcal/mol for both nitrogen molecules combined (Table 2). The elongation of the two nitrogen molecules causes a much smaller energy increase: $\Delta E_{prep,geo} = 29.2$ kcal/mol.

The sum of the valence excitation and deformation energy, $\Delta E_{prep,el} + \Delta E_{prep,geo} = 307.8$ kcal/mol, can be taken as an upper bound for the activation energy of the cycloaddition step (see eq 4), but the actual barrier is probably much lower (vide infra).

The net N_2-N_2 interaction ΔE_{int} of −133.9 kcal/mol is mainly provided by the $1\pi_{u,x} - 1\pi_{u,x}$ and $1\pi_{g,x} + 1\pi_{g,x}$ electron-pair bonds (Figure 5, left); in line with its σ character, the buildup of overlap between the occupied $1\pi_{u,x}$ orbitals of the two dinitrogen fragments (0.25) is far ahead of the π type overlaps between the $1\pi_{u,y}$ (0.16) and the $3\sigma_g$ (0.16) orbitals (Table 2). The two electron-pair bonds cannot compensate for the high electronic preparation energy associated with the level crossing. This leads overall to an extremely high endothermicity for the formation of **2a** from $2N_2$: $\Delta E = \Delta E_{prep,el} + \Delta E_{prep,geo} + \Delta E_{int} = 173.9$ kcal/mol (for **2**, this would be 166.7 kcal/mol, Table 1).

Compare this with the endothermicity of 52.2 kcal/mol for the formation of $\mathbf{2}^+$ from $N_2 + N_2^+$. The stabilization by more than a factor of 3 can be traced to the very low excitation energy, only 16.9 kcal/mol,[19] required to bring N_2^+ into its valence configuration N_2^+* (Table 2). In the process, a bonding $1\pi_{u,x}$ electron has to be excited only to the essentially nonbonding, low-energy $3\sigma_g$ SOMO instead of the high-energy antibonding $1\pi_{g,x}$ (Figure 4). The combined excitation energies of N_2 and N_2^+ ($\Delta E_{prep,el} = 156.2$ kcal/mol) are 122.4 kcal/mol under those of $2N_2$. The sum of the valence excitation and deformation energy, $\Delta E_{prep,el} + \Delta E_{prep,geo} = 181.9$ kcal/mol, an upper bound for the activation energy of the cationic cycloaddition step, is also much lower than that for the neutral one (307.8 kcal/mol).

At this point, it is interesting to note that the valence excitation energy mentioned above also plays a key role in the curve-crossing model (schematically illustrated in Figure 6), proposed by Shaik for understanding barrier formation in chemical reactions.[20] The valence excitation energy corresponds to the energy gap *G* in Shaik's model between the reactant (Ψ_R) and product configuration (Ψ_P). In the reactants, Ψ_R is the ground state of the system, whereas Ψ_P is an excited state at an energy *G* above Ψ_R. Let's take $N_2 + N_2$ in reaction 4 as an example (Figure 6a): here, Ψ_R is the ground-state configuration of two nitrogen molecules and Ψ_P corresponds to the configuration of these molecules after $\pi-\pi^*$ excitation (see Figure 4). As the reaction proceeds, the energy of Ψ_R rises and that of Ψ_P drops. The transition state is reached at a point along the reaction coordinate where the energy curves of Ψ_R and Ψ_P cross. The reaction system reaches a maximum energy somewhat below the crossing point, due to $\Psi_R-\Psi_P$ configuration mixing near the transition state or, in other words, an avoided crossing; this is indicated by the dotted curves in Figure 6. Finally, in the products the roles of Ψ_R and Ψ_P have been inverted: Ψ_P has become the ground-state configuration and Ψ_R an excited state. In our example, Ψ_P has been turned into the ground-state configuration of tetraazacyclobutadiene **2** and Ψ_P corresponds to a doubly excited state of this intermediate.

Now, if one reduces *G*, curve crossing occurs at a lower energy, leading to a lower barrier (Figure 6b). Such a reduction of the energy gap *G* is exactly what happens on ionization of $N_2 + N_2$, as has been discussed above (see Figure 4).

We can use this model for estimating the actual barriers of the cycloaddition of $N_2 + N_2$ (eq 4) and $N_2 + N_2^+$ by making the crude assumption that the curves of Ψ_R and Ψ_P cross at an energy $0.5G$ and substituting $G = \Delta E_{prep,el} + \Delta E_{prep,geo}$. This yields the approximate values of 154 and 91 kcal/mol for the barriers of the neutral (eq 4) and cationic cycloaddition steps, respectively. The value of 154 kcal/mol for the neutral reaction is below that of one of the energy minima (**2**, 166.7 kcal/mol) connected by the TS; this is obviously too low. A better estimate for the cycloaddition barrier of eq 4 is probably obtained by adding the CASSCF(8,8) electronic activation energy for the reverse reaction (5.6 kcal/mol)[12m] to our energy for **2**, which yields 172.3 kcal/mol.

We wish to emphasize that "configuration curve crossing" and "orbital level crossing" are closely related concepts, describing the same phenomenon from slightly different perspectives. Shaik's curve-crossing model focuses on the electronic configurations of a system and emerges naturally from a valence bond (VB) approach. The concept of orbital level crossings highlights the role of individual one-electron functions or orbitals and evolves just as naturally from molecular orbital (MO) theory.

E. Alternative Mechanisms for $N_2 + N_2^+$ Nitrogen Exchange. Our results suggest that ionization significantly

lowers the barrier to nitrogen exchange. Yet, a reaction involving intermediate $\mathbf{2}^+$ (52.2 kcal/mol) and a D_{4h} symmetric transition state (≥102.9 kcal/mol, $\mathbf{1}^+$) still has a very high barrier. We have investigated some other plausible geometrical arrangements for reaction, also allowing for lower[8b] point group symmetries: **1**−**10** and $\mathbf{1}^+$−$\mathbf{10}^+$ (Figure 3). We emphasize, however, that a comprehensive exploration of the potential energy surface is beyond the scope of this investigation.

The NL-SCF/TZ2P energies of **1**−**10**, relative to **3**, are in reasonable agreement with the MP4SDTQ and G2 values (Table 1). The reactants $N_2 + N_2$ are, however, significantly more stable at MP4SDTQ and G2 levels of computation than in our results, namely by 24.9 and 19.5 kcal/mol. Our NL-SCF/TZ2P ionization energy for N_2 (355.8 kcal/mol) is 3.5 kcal/mol lower than the experimental value (359.3 kcal/mol).[18b] Triplet N_2-($^3\Sigma_u^+$), approximated with a $|...\pi_x(1)\alpha(1)\ \pi_x^*(2)\alpha(2)|$ configuration, is 148.9 kcal/mol higher in energy than ground-state $N_2(^1\Sigma_g^+)$ at NL-SCF/TZ2P (experimental value:[18b] 143.5 kcal/mol). We find $N_2^+(^2\Pi_u)$, approximated with a $|...\pi_x(1)\alpha(1)\ \pi_y(2)\alpha(2)\ \pi_y(3)\beta(3)|$ configuration, 27.3 kcal/mol above ground-state $N_2^+(^2\Sigma_g^+)$, only 1 kcal/mol higher than the experimental excitation energy of 26.2 kcal/mol.[18b]

All structures studied are still too high in energy to serve as intermediates in a "low-barrier" exchange reaction (Table 1). The tetraazatetrahedrane cation $\mathbf{3}^+$, the D_{3h} symmetric $\mathbf{5}^+$, and the Y-shaped $\mathbf{9}^+$ cations are 127.9, 138.6, and 35.4 kcal/mol above $N_2 + N_2^+$ (for comparison, the neutral **3**, **5**, and **9** are at 157.9, 226.5, and 171.3 kcal/mol with respect to $2N_2$, the global minimum of the N_4 systems studied).

Only the linear $D_{\infty h}$ symmetric $\mathbf{10}^+$ is strongly bound with respect to $N_2 + N_2^+$, by a 2c−3e bond of −46.7 kcal/mol. Yet, it does not have the right geometrical arrangement to yield nitrogen exchange.[18] On the basis of the low energy of the radical cation dimer $\mathbf{10}^+$, we have further investigated the possibility of a low-energy rearrangement via a termolecular process in which $\mathbf{10}^+$ binds another N_2 and then forms a six-membered-ring structure (eq 6).

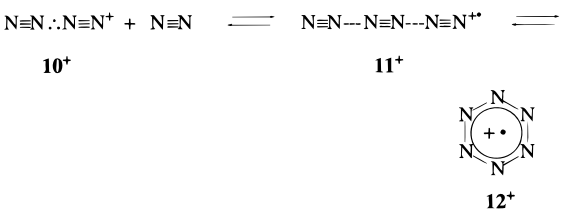

(6)

The linear, "termolecular" intermediate $\mathbf{11}^+$ turns out to be at −17.3 kcal/mol relative to $\mathbf{10}^+ + N_2$ (NL-SCF/TZ2P) and extremely floppy with doubly degenerate, symmetric bending modes with associated frequencies of only 5 cm^{-1}. The six-membered ring $\mathbf{12}^+$, however, is again 70.0 kcal/mol higher in energy than $2N_2 + N_2^+$ or 116.7 kcal/mol above $\mathbf{10}^+ + N_2$. This cyclic structure cannot be involved in a low-energy pathway for nitrogen exchange.

We have also investigated a bimolecular mechanism for cationic nitrogen exchange, proceeding via a C_{2v} symmetric, T-shaped transition state. The fact that the Y-shaped $\mathbf{9}^+$ is lower in energy than intermediate $\mathbf{2}^+$ suggests namely that such an alternative mechanism could be competitive with the least-motion process for exchange (vide supra). However, $\mathbf{9}^+$ itself is not involved as an intermediate or transition state in such an alternative mechanism. It is a transition state for internal rotation of one N_2 unit with respect to the other, $\mathbf{10}^+ \rightarrow \mathbf{9}^+ \rightarrow \mathbf{10}^+$. The T-shaped transition state, **TS**(C_{2v}), which leads to nitrogen exchange is shown below (the arrows indicate the transition vector[21] associated with the imaginary frequency of i939 cm^{-1}):

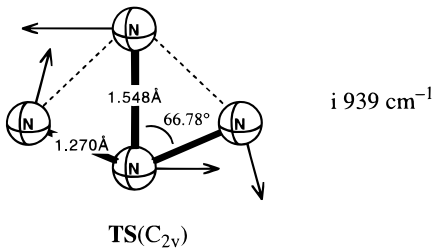

TS(C_{2v})

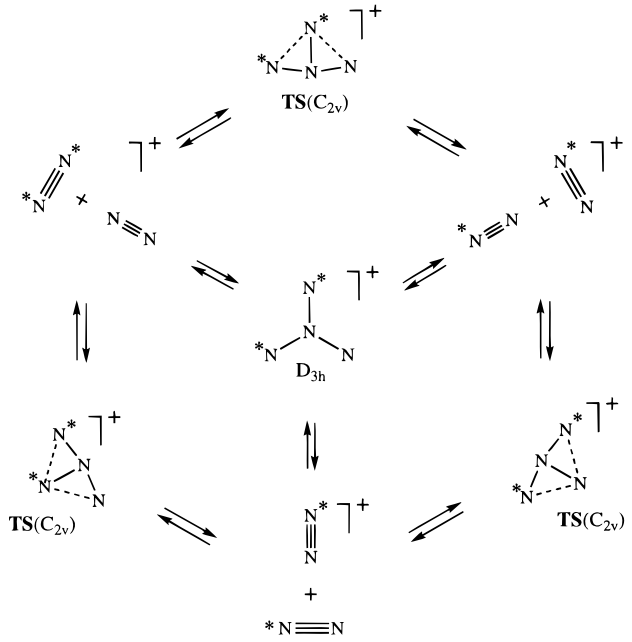

Figure 7. Alternative mechanism for $N_2 + N_2^+$ nitrogen exchange, involving C_{2v} symmetric, T-shaped transition states **TS**(C_{2v}). Here, * marks an isotopic label. A D_{3h} symmetric saddle point (center) is, by symmetry, of second order and higher in energy than **TS**(C_{2v}).

TS(C_{2v}) is 102.8 kcal/mol above the reactants $N_2 + N_2^+$. This barrier indeed is in the same order as the lower bound for that of the isomerization of $\mathbf{2}^+$ via $\mathbf{1}^+$ into $\mathbf{2'}^+$ (102.9 kcal/mol above $N_2 + N_2^+$, Table 1). From the transition vector (see above), it follows that **TS**(C_{2v}) connects two linear complexes $\mathbf{10}^+$ via a path in which $\mathbf{9}^+$ is avoided, as shown in Scheme 1 (where * marks an isotopic label).[22]

Finally, one could also imagine a D_{3h} symmetric structure being involved in $N_2 + N_2^+$ nitrogen exchange (see Figure 7). However, by symmetry, this highly symmetric species would have a doubly degenerate transition vector[21] and would, therefore, be a *second-order* saddle point, connecting three equivalent minima $\mathbf{10}^+$, as shown in Figure 7. As pointed out by McIver et al.,[23] there will always be a *first-order* saddle point at lower energy, like our **TS**(C_{2v}), connecting only two minima $\mathbf{10}^+$. The DFT calculations show that indeed the energy of the quartet species $\mathbf{5}^+$, 138.6 kcal/mol (Table 1), a lower bound for that of the D_{3h} symmetric second-order saddle point, is higher than the energy of **TS**(C_{2v}), 102.8 kcal/mol.

4. Conclusion

The hypothetical four-center nitrogen exchange reaction of two N_2 molecules, approaching in a parallel manner with D_{2h} symmetry (eq 1), has a very high activation barrier. Simple molecular orbital arguments suggest that ionization of the

SCHEME 1

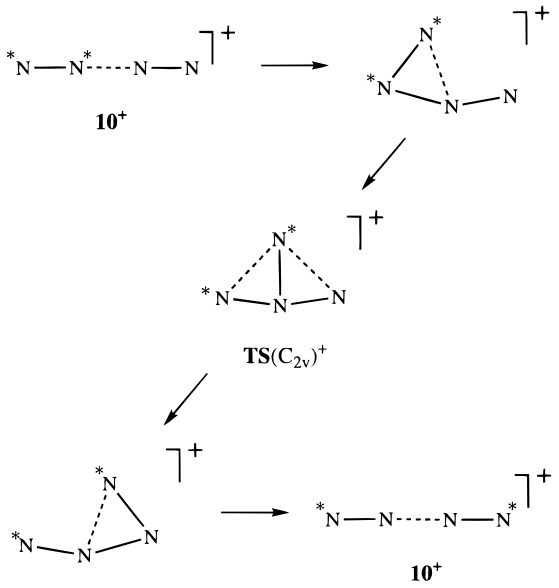

reaction system (eq 5) significantly lowers this barrier. This is supported by nonlocal density functional calculations. However, the DFT calculations also indicate that the barrier of the thermal $N_2 + N_2^+$ reaction is still at high energy. They also suggest that if the $N_2 + N_2^+$ reaction occurs at all, a mechanism involving a T-shaped transition state may be competitive with the least-motion process.

A detailed analysis of the electronic structure reveals that the three level crossings accompanying the least-motion nitrogen exchange reaction occur at different points along the reaction coordinate. One of the reasons is the different rates at which the N_2 fragment orbitals, involved in different crossings, are building up overlap, σ type interactions running ahead of π type interactions. This leads to a mechanism involving three "singly forbidden" reaction steps and two tetraazacyclobutadiene intermediates. The overall reaction too may therefore be considered only "singly" and *not* "triply forbidden".

Ionization removes an electron from the system and reduces the energy demand associated with the very high-energy empty−occupied level crossings of the first and last reaction step which become formally "half-forbidden". This effect dominates a slight increase of the smaller barrier for the second step, which becomes formally "1.5-fold forbidden" because here the electron is not removed from the empty−occupied level crossing but from two occupied, crossing lone-pair orbitals. Overall, the least-motion $N_2 + N_2^+$ reaction is effectively only "half as forbidden" as the corresponding neutral process.

Yet, the experimental realization of the $N_2 + N_2^+$ reaction can, according to our results, only be achieved at high-energy collisions or via excitation of the reactants, in particular of N_2. A useful first step in tackling this *experimental* challenge, and an interesting extension of our work, could be a comprehensive *theoretical* exploration of the potential energy surfaces of both reaction systems, $N_2 + N_2$ and $N_2 + N_2^+$.

Acknowledgment. We would like to thank Prof. Dr. S. S. Shaik for helpful discussions. This work was supported by the National Science Foundation (NSF) and the Deutsche Forschungsgemeinschaft (DFG). F.M.B. gratefully acknowledges a postdoctoral DFG fellowship. We are also grateful to the Theory Center of Cornell University (Research Grant 546) and The Netherlands Organization for Scientific Research (NCF/NWO) for their support of our work.

References and Notes

(1) King, D. L.; Herschbach, D. R. *Discuss. Faraday Soc.* **1973**, *55*, 331.

(2) (a) Houk, K. N.; Li, Y.; Evanseck, J. D. *Angew. Chem.* **1992**, *104*, 711; *Angew. Chem., Int. Ed. Engl.* **1992**, *31*, 682. (b) Hoffmann, R.; Swaminathan, S.; Odell, B. G.; Gleiter, R. *J. Am. Chem. Soc.* **1970**, *92*, *2*, 7091.

(3) (a) Horn, B. A.; Herek, J. L.; Zewail, A. H. *J. Am. Chem. Soc.* **1996**, *118*, 8755. (b) Raz, T.; Levine, R. D. *J. Phys. Chem.* **1995**, *99*, 13713. (c) Berson, J. A. *Science* **1994**, *266*, 1338. (d) Pedersen, S.; Herek, J. L.; Zewail, A. H. *Science* **1994**, *266*, 1359.

(4) Flynn, G. W.; Weston, R. E., Jr. *Annu. Rev. Phys. Chem.* **1986**, *37*, 551.

(5) (a) Rubahn, H.-G.; Bergmann, K. *Annu. Rev. Phys. Chem.* **1990**, *41*, 735. (b) Yang, X.; Wodtke, A. M. *Int. Rev. Phys. Chem.* **1993**, *12*, 123.

(6) Raz, T.; Levine, R. D. *J. Phys. Chem.* **1995**, *99*, 7495.

(7) (a) Schultz, R. H.; Armentrout, P. B. *J. Chem. Phys.* **1992**, *96*, 1046. (b) Farrar, J. M. *Annu. Rev. Phys. Chem.* **1995**, *46*, 525.

(8) (a) For an extensive discussion of the rules of orbital symmetry as well as symmetry-forbidden and -allowed reactions, see: Woodward, R. B.; Hoffmann, R. *Angew. Chem.* **1969**, *81*, 797. (b) See also: Hoffmann, R. *J. Chem. Phys.* **1968**, *49*, 3739.

(9) Albright, T. A.; Burdett, J. K.; Whangbo, M.-H. *Orbital Interactions in Chemistry*; Wiley-Interscience: New York, 1985.

(10) (a) Knott, W. J.; Proch, D.; Kompa, K. L.; Rose-Petruck, Ch. *J. Chem. Phys.* **1995**, *102*, 214. (b) Uiterwaal, C. J. G. J.; van Eck, J.; Niehaus, A. *J. Chem. Phys.* **1995**, *102*, 744. (c) Dubernet, M. L.; Rebentrost, F.; Kompa, K. L.; Levine, R. D. *J. Chem. Phys.* **1996**, *105*, 953.

(11) (a) Sun, Q.; Yang, D. L.; Wang, N. S.; Bowman, J. M.; Lin M. C. *J. Chem. Phys.* **1990**, *93*, 4730. (b) Wright, S. A.; Dagdigian, P. J. *J. Chem. Phys.* **1995**, *103*, 6479. (c) Mohammad, F.; Morris, V. R.; Fink, W. H.; Jackson, W. M. *J. Phys. Chem.* **1993**, *97*, 11590.

(12) (a) Korkin, A. A.; Balkova, A.; Bartlett, R. J.; Boyd, R. J.; Schleyer, P. v. R. *J. Phys. Chem.* **1996**, *100*, 5702. (b) Glukhovtsev, M. N.; Laiter, S. *J. Phys. Chem.* **1996**, *100*, 1569. (c) Gimarc, B. M.; Zhao, M. *Inorg. Chem.* **1996**, *35*, 3289. (d) Glukhovtsev, M. N.; Laiter, S.; Pross, A. *J. Phys. Chem.* **1995**, *99*, 6828. (e) Dunn, K. M.; Morokuma, K. *J. Chem. Phys.* **1995**, *102*, 4904. (f) Glukhovtsev, M. N.; Schleyer, P. v. R. *Int. J. Quantum Chem.* **1993**, *46*, 119. (g) Lauderdale, W. J.; Stanton, J. F.; Bartlett, R. J. *J. Phys. Chem.* **1992**, *96*, 1173. (h) Murray, J. S.; Seminario, J. M.; Lane, P.; Politzer, P. *J. Mol. Struct. (THEOCHEM)* **1990**, *207*, 193. (i) de Castro, S. C.; Schaefer, H. F. *J. Chem. Phys.* **1981**, *74*, 550. (j) Yarkony, D. R. *J. Am. Chem. Soc.* **1992**, *114*, 5406. (k) Lee, T. J.; Rice, J. E. *J. Chem. Phys.* **1991**, *94*, 1215. (l) Francl, M. M.; Chesik, J. P. *J. Phys. Chem.* **1990**, *94*, 526, and references therein. (m) Larson, Å.; Larsson, M.; Östmark, M. *J. Chem. Soc., Faraday Trans.* **1997**, *93*, 2963.

(13) (a) Norwood, K.; Luo, G.; Ng, C. Y. *J. Chem. Phys.* **1989**, *91*, 849. (b) Hiraoka K.; Nakajima, G. *J. Chem. Phys.* **1988**, *88*, 7709. (c) Smith, G. P.; Lee, L. C. *J. Chem. Phys.* **1978**, *69*, 5393.

(14) (a) Kemister, G.; Peel, J. B. *Org. Mass Spectrom.* **1993**, *28*, 311. (b) Carmichael, I. *J. Phys. Chem.* **1994**, *98*, 5044. (c) Frecer, V.; Jain, D. C.; Sapse, A.-M. *J. Phys. Chem.* **1991**, *95*, 9263. (d) Knight, L. B., Jr.; Johannessen, K. D.; Cobranchi, D. C.; Earl, E. A. *J. Chem. Phys.* **1987**, *87*, 885. (e) de Castro, S.; Schaefer, H. F. *J. Chem. Phys.* **1981**, *74*, 550. (f) Conway, D. C. *J. Chem. Phys.* **1975**, *63*, 2219.

(15) (a) Parr, R. G.; Yang, W. *Density-Functional Theory of Atoms and Molecules*; Oxford University Press: New York, 1989. (b) Slater, J. C. *Quantum Theory of Molecules and Solids*; McGraw-Hill: New York, 1974; Vol. 4.

(16) (a) Fonseca Guerra, C.; Visser, O.; Snijders, J. G.; te Velde, G.; Baerends, E. J. In *Methods and Techniques for Computational Chemistry*; Clementi, E., Corongiu, G., Eds.; STEF: Cagliari, Italy, 1995; pp 305−395, and references therein. (b) Baerends, E. J.; Ellis, D. E.; Ros, P. *Chem. Phys.* **1973**, *2*, 41. (c) Snijders, J. G.; Baerends, E. J.; Vernooijs, P. *At. Nucl. Data Tables* **1982**, *26*, 483. (d) Boerrigter, P. M.; te Velde, G.; Baerends, E. J. *Int. J. Quantum Chem.* **1988**, *33*, 87. (e) Vosko, S. H.; Wilk, L.; Nusair, M. *Can. J. Phys.* **1980**, *58*, 1200. (f) Becke, A. D. *J. Chem. Phys.* **1986**, *84*, 4524. (g) Becke, A. D. *Phys. Rev. A* **1988**, *38*, 3098. (h) Perdew, J. P. *Phys. Rev. B* **1986**, *33*, 8822. Erratum: *Ibid.* **1986**, *34*, 7406. (i) Fan, L.; Ziegler, T. *J. Chem. Phys.* **1991**, *94*, 6057.

(17) (a) Bickelhaupt, F. M.; Nibbering, N. M. M.; van Wezenbeek, E. M.; Baerends, E. J. *J. Phys. Chem.* **1992**, *96*, 4864. (b) Ziegler, T.; Rauk, A. *Theoret. Chim. Acta* **1977**, *46*, 1. (c) In case of open-shell fragments, the ETS analysis yields for technical reasons an interaction energy that differs consistently by a few kcal/mol from the more accurate $\Delta E_{int} = E_{molecule} - \sum E_{fragments}$ obtained in regular calculations with respect to atoms. To facilitate a straightforward comparison, the results of the analysis are scaled to match exactly the regular bond energies. See also, for example: (d) Morokuma, K. *J. Chem. Phys.* **1971**, *55*, 1236. (e) Kitaura, K.; Morokuma, K. *Int. J. Quantum. Chem.* **1976**, *10*, 325.

(18) (a) Also, a possible coaxial (or other) arrangement must eventually undergo a rearrangement via structures such as **1**−**9** in order to yield nitrogen exchange. Exchange mechanisms of the type $N_2 + N_2 \rightarrow [N_2 + 2N \rightarrow] N_3$

+ N → N_2 + N_2, involving two separate collisions, are energetically also highly unfavorable: (a) the experimental N_2 bond dissociation energy is 225.1 kcal/mol (ref 18b) and N_3 (doublet state) + N is 204.3 kcal/mol above N_2 + N_2 (NL-SCF/TZ2P). (b) Huber, K. P.; Herzberg, G. *Molecular Spectra and Molecular Structure*; Van Nostrand Reinhold: New York, 1979; Vol. 4, p 412.

(19) This value refers to the vertical excitation of the elongated N_2^+ fragment in $\mathbf{2}^+$. The *adiabatic* $^2\Sigma_g \rightarrow {}^2\Pi_u$ excitation energy for N_2^+ is somewhat higher: 31.4 kcal/mol.

(20) (a) Shaik, S. S. *J. Am. Chem. Soc.* **1981**, *103*, 3692. (b) Pross, A.; Shaik, S. S. *Acc. Chem. Res* **1983**, *16*, 363. (c) Shaik, S. S.; Schlegel, H. B.; Wolfe, S. *Theoretical Aspects of Physical Organic Chemistry*; Wiley: New York, 1992, Chapter 3. (d) Shaik, S.; Hiberty, P. C. *Adv. Quantum Chem.* **1995**, *26*, 99.

(21) The transition vector is the normal mode connecting reactants and products. It is an eigenvector of the force constant matrix associated with a negative eigenvalue.

(22) This is also confirmed by allowing **TS**(C_{2v}), after a slight geometric distortion, to relax to an equilibrium structure, which indeed turns out to be $\mathbf{10}^+$.

(23) (a) McIver, J. W., Jr. *Acc. Chem. Res* **1974**, *7*, 72. (b) Stanton, R. E.; McIver, J. W., Jr. *J. Am. Chem. Soc.* **1975**, *97*, 3632.